Current Biology 21, 967–974, June 7, 2011 ©2011 Elsevier Ltd All rights reserved DOI 10.1016/j.cub.2011.04.030

Report

Rab6, Rab8, and MICAL3 Cooperate in Controlling Docking and Fusion of Exocytotic Carriers

Ilya Grigoriev,[1,8,9] Ka Lou Yu,[1,8] Emma Martinez-Sanchez,[2,8] Andrea Serra-Marques,[1,9] Ihor Smal,[3] Erik Meijering,[3] Jeroen Demmers,[4] Johan Peränen,[5] R. Jeroen Pasterkamp,[6] Peter van der Sluijs,[2] Casper C. Hoogenraad,[7,9] and Anna Akhmanova[1,9,*]

[1]Department of Cell Biology, Erasmus Medical Center, PO Box 2040, 3000 CA Rotterdam, The Netherlands
[2]Department of Cell Biology, University Medical Center Utrecht, 3584 CX Utrecht, The Netherlands
[3]Biomedical Imaging Group Rotterdam, Department of Medical Informatics and Radiology, Erasmus Medical Center, PO Box 2040, 3000 CA Rotterdam, The Netherlands
[4]Proteomics Center, Erasmus Medical Center, 3015 GE Rotterdam, The Netherlands
[5]Institute of Biotechnology, University of Helsinki, PO Box 56, Viikinkaari 9, FIN-00014, Finland
[6]Department of Neuroscience and Pharmacology, Rudolf Magnus Institute of Neuroscience, University Medical Center Utrecht, 3584 CG Utrecht, The Netherlands
[7]Department of Neuroscience, Erasmus Medical Center, 3015 GE Rotterdam, The Netherlands

Summary

Rab6 is a conserved small GTPase that localizes to the Golgi apparatus and cytoplasmic vesicles and controls transport and fusion of secretory carriers [1]. Another Rab implicated in trafficking from the trans-Golgi to the plasma membrane is Rab8 [2–5]. Here we show that Rab8A stably associates with exocytotic vesicles in a Rab6-dependent manner. Rab8A function is not needed for budding or motility of exocytotic carriers but is required for their docking and fusion. These processes also depend on the Rab6-interacting cortical factor ELKS [1], suggesting that Rab8A and ELKS act in the same pathway. We show that Rab8A and ELKS can be linked by MICAL3, a member of the MICAL family of flavoprotein monooxygenases [6]. Expression of a MICAL3 mutant with an inactive monooxygenase domain resulted in a strong accumulation of secretory vesicles that were docked at the cell cortex but failed to fuse with the plasma membrane, an effect that correlated with the strongly reduced mobility of MICAL3. We propose that the monooxygenase activity of MICAL3 is required to regulate its own turnover and the concomitant remodeling of vesicle-docking protein complexes in which it is engaged. Taken together, the results of our study illustrate cooperation of two Rab proteins in constitutive exocytosis and implicates a redox enzyme in this process.

Results and Discussion

Small GTPase Rab6 is associated with the Golgi complex and cytoplasmic vesicles; it is represented in mammals by Rab6A and Rab6A′, which are ubiquitously expressed and will be collectively called Rab6 here when referring to the endogenous protein, and the neuronal isoform Rab6B [7–10]. In nonpolarized cells such as HeLa, the majority of Rab6 vesicles are constitutive secretion carriers [1]. Because Rab8 has also been implicated in secretory traffic [2–5], we tested whether endogenous Rab6 and Rab8A colocalize on the same vesicles and found that this was indeed the case (Figures 1A and 1B). Rab8A-positive vesicles are exocytotic carriers because they contain the secretion marker neuropeptide Y (NPY)-Venus [1, 11] (Figure 1C). In addition, antibodies against Rab8A weakly stain the Golgi region and strongly decorate tubules, which show strong variability in size and abundance and likely represent an endosomal compartment [5, 12]. These tubules were devoid of endogenous Rab6 or NPY-Venus (arrows in Figures 1A and 1L; Figure 2E).

Next, we analyzed Rab6A-Rab8A colocalization by live imaging and found a high degree of overlap between the two markers on vesicles (Figures 1D and 1E). Colocalization of the two Rabs on moving vesicles was observed from the moment the vesicles left the Golgi area (Figure 1H; see also Figures S1A and S1B available online). Similar results were obtained in other cell lines, such as MRC5-SV (data not shown) and hTert-RPE1 (Figures S1C and S1D). Importantly, in serum-starved hTert-RPE1 cells, mStrawberry-Rab8A strongly accumulated in the primary cilia, in line with the published data [13], whereas GFP-Rab6 was not enriched in cilia (Figure S1C).

To investigate at which point Rab8A was recruited to secretory vesicles, we used Rab8A fused to photoactivatable GFP [14] (PAGFP-Rab8A) in combination with the Golgi marker mCherry-galactosyl transferase (GT) or mStrawberry-Rab6A. When PAGFP-Rab8A was photoactivated in the Golgi area, we observed weak fluorescence of the Golgi stacks and bright vesicles that rapidly moved away from the Golgi membranes to the cell periphery (Figures 1F and 1G; Movie S1). These vesicles were positive for mStrawberry-Rab6 (data not shown). Photoactivation of other cell regions visualized PAGFP-Rab8A-labeled vesicles that moved to the cell periphery where they disappeared (Movie S2). PAGFP-Rab8A-positive but Rab6A-negative tubular structures were also present in some cells (Movie S2); importantly, we never observed fusion of such structures to Rab6A-positive vesicles.

Using *f*luorescence *r*ecovery *a*fter *p*hotobleaching (FRAP) assay, we have shown that Rab6A does not significantly exchange on exocytotic vesicles [1], and we found that the same was true for Rab8A (Figure S1E and S1F). In line with this result, when PAGFP-Rab8A was photoactivated on vesicles, no significant fluorescence loss was observed within 30 s (Figures 1I and 1J), which is approximately one-third of the ~100 s duration of the exocytotic vesicle life cycle.

Next, we examined Rab8A behavior in the vicinity of the plasma membrane by using dual-color live *t*otal *i*nternal *r*eflection *f*luorescence *m*icroscopy (TIRFM). Before PAGFP-Rab8A/mStrawberry-Rab6A double-positive vesicles disappeared, they displayed a simultaneous increase of the green and red fluorescence followed by lateral diffusion of the two markers, as expected for a plasma membrane fusion event [15] (Figures 1I and 1K; Movie S2). Taken together, our data show that

[8]These authors contributed equally to this work
[9]Present address: Division of Cell Biology, Faculty of Science, Utrecht University, Padualaan 8, 3584 CH Utrecht, The Netherlands
*Correspondence: a.akhmanova@uu.nl

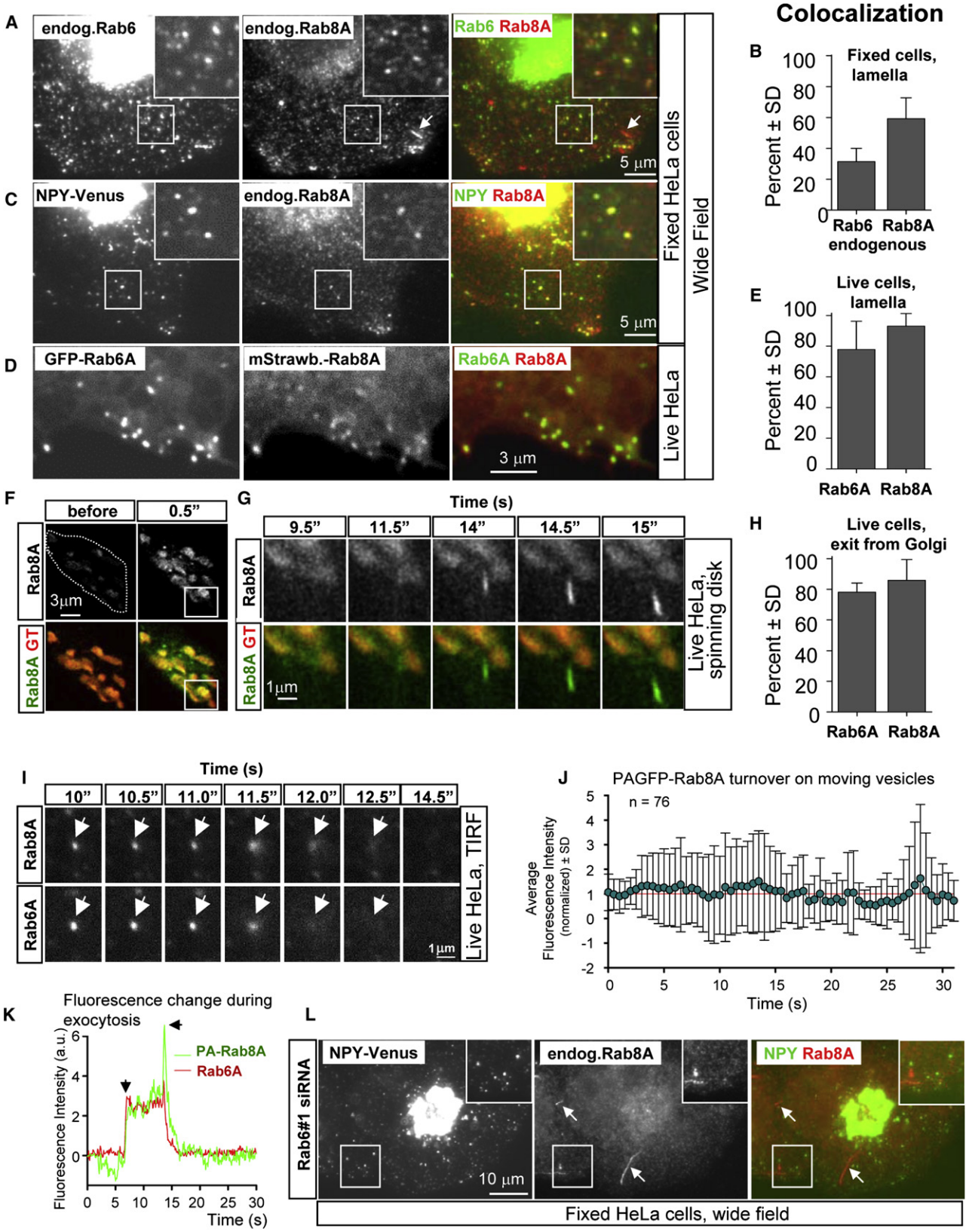

Figure 1. Rab8A Binds to Exocytotic Carriers in a Rab6-Dependent Manner

(A) HeLa cells were stained for endogenous Rab6 and Rab8A.

(B, E, and H) Quantification of colocalization of Rab6 and Rab8A in HeLa cells. (B) Colocalization of endogenous Rab6 and Rab8; note that because of the relatively high cytosolic Rab8A background, it was difficult to distinguish weak vesicular Rab8A staining, and the numbers for the endogenous proteins likely represent an underestimate. (E and H) Colocalization of Rab6A and Rab8A in live-cell images on vesicles in cell lamella or exiting the Golgi, respectively.

Rab8A is present on Rab6-negative membrane compartments, such as cytoplasmic tubules and cilia, and Rab6-positive exocytotic vesicles. Rab8A is loaded on these vesicles during or soon after their exit from the Golgi and displays little turnover until the vesicles fuse with the plasma membrane.

Rab6 depletion alters the behavior of exocytotic carriers but does not prevent their formation [1]. Interestingly, although Rab6 knockdown had no effect on Rab8A expression (Figure S1G), it caused a complete loss of both endogenous and fluorescently tagged Rab8A from NPY-Venus-positive exocytotic vesicles (Figure 1L; Figure S1H). We conclude that Rab6 is required for Rab8A recruitment to the secretory vesicle membrane. We have tested whether this was due to a direct interaction between Rab6 and Rab8 GEFs Rabin3/Rabin8 and Rabin3-like/GRAB [16, 17] but found no evidence supporting this idea (data not shown).

Next, we investigated whether the interference with Rab8A function by expressing Rab8 mutants would affect the behavior of Rab6 vesicles. Whereas overexpression of the GTP-bound Rab8A-Q67L caused a slight decrease in the number of endogenous Rab6 vesicles, the expression of GDP-bound Rab8A-T22N caused a strong increase in vesicle number at the cell margin (Figures 2A–2C and 2G). A small interfering RNA (siRNA)-mediated depletion of Rab8A also caused an increase in the number of vesicles (Figures 2D and 2G) without affecting Rab6 expression (Figure S1G). Peripherally accumulated Rab6 vesicles contained exocytotic marker NPY-Venus (Figure 2D), indicating that Rab6 recruitment to secretory vesicles is Rab8A independent. The specificity of the effect of Rab8 depletion could be confirmed by rescue with low-level expression of the GFP-Rab8A insensitive to the siRNAs used (Figure S2A).

To confirm the involvement of Rab8A in constitutive secretion, we used a flow cytometry-based assay [18], which employs a secreted GFP-tagged reporter protein that is aggregated and retained in the endoplasmic reticulum (ER) but becomes soluble and is rapidly secreted when a cell-permeable ligand is added. Using this assay, we observed a relatively mild but significant secretion delay in Rab8A-depleted cells and a stronger secretion defect in Rab6-depleted cells (Figure 2F). The latter was possibly due to defects in Golgi function and/or vesicle fission [19].

Using HeLa cells stably expressing GFP-Rab6A [1], we found that interference with Rab8A function had no significant effect on the frequency of emergence of GFP-Rab6A vesicles from the Golgi, or on their movement (Figures S2B–S2D). In contrast, whereas in control cells, Rab6 vesicles underwent rapid docking followed by fusion with the plasma membrane, which occurred within ~30 s after initial immobilization, in Rab8A-depleted cells, GFP-Rab6A vesicles underwent diffusive movements at the cell margin, and the duration of the pause between final immobilization and actual fusion with plasma membrane (terminal pause) was strongly increased (Figure 2H; Figures S2E, S2F, and S2H). Previously, we observed a similar defect in docking and fusion of Rab6 vesicles in cells depleted of the cortical Rab6-interacting coiled-coil protein ELKS (also known as ERC1, CAST2, or Rab6IP2) [1, 20]. Using ELKS siRNA, we showed that ELKS is not required for Rab8A recruitment to Rab6 vesicles (Figure 2E). Furthermore, we confirmed our previous results showing that ELKS had no effect on Rab6 vesicle emergence from the Golgi or their microtubule-based movement (Figures S2B–S2D) but was needed for their proper docking and fusion (Figure 2H; Figures S2F and S2H) and caused a reduction in secretion efficiency similar to Rab8A depletion (Figure 2F).

Our results suggest that Rab8A and ELKS might work in the same pathway. We could detect no significant pool of ELKS on the vesicles (data not shown). Instead, ELKS localized to patches at the cell cortex, and these patches served as sites for preferential docking and fusion of Rab6 vesicles [1, 21]. In Rab8A-depleted cells, Rab6 vesicles preferentially accumulated in regions devoid of cortical ELKS (Figure S2I), indicating that Rab8A might contribute to vesicle interaction with ELKS-positive sites at the plasma membrane. However, we could find no strong evidence for a direct binding between Rab8A and ELKS (data not shown).

To search for proteins that could link Rab8A and ELKS, we performed pull-down assays with biotinylation and GFP-tagged (BioGFP) ELKS (Figure S3A) and analyzed the resulting proteins by mass spectrometry. One of the most significant hits was MICAL3 (Figures S3B and S3C), a member of the MICAL family of flavoprotein monooxygenases implicated in axon guidance and actin remodeling [6, 22, 23]. MICALs, encoded in mammals by three genes, are large proteins, which, in addition to the monooxygenase enzymatic domain, include an actin-binding calponin homology (CH) domain, a LIM domain, and several predicted coiled coils (Figure 3A). There are also two MICAL-like proteins, which lack the monooxygenase domain [24]. The C-terminal domains of MICAL1, MICAL2 (MICAL-cl), and MICAL-L1/L2 were shown to interact with Rab8A as well as some other Rabs [24, 25]. We confirmed the Rab8A-MICAL1 binding and showed that MICAL3 also interacts with Rab8A through its C terminus (Figure 3B), an interaction that was previously overlooked because an incomplete MICAL3 cDNA was tested [24].

We raised antibodies against MICAL3 and showed that the full-length protein is expressed in HeLa cells (Figure S3D).

Left bar, Rab6 vesicles showing strong Rab8A labeling; right bar, Rab8A vesicles showing strong Rab6 labeling. Numbers of counted vesicles: endogenous Rab6/Rab8A, 1234 vesicles in 15 cells; Rab6A/Rab8A vesicles in lamella, 739 vesicles in 6 cells; Rab6A/Rab8A vesicles exiting the Golgi, 259 vesicles in 7 cells.

(C) HeLa cells, stably expressing NPY-Venus, were stained for endogenous Rab8A.

(D) Representative frames of a simultaneous two-color movie, showing the periphery of a HeLa cell expressing GFP-Rab6A and mStrawberry-Rab8A.

(F and G) Frames from a simultaneous two-color movie, showing the Golgi area of a HeLa cell expressing PAGFP-Rab8A (green) and mCherry-GT (red). The area indicated with a stippled line was photoactivated using a 408 nm laser. Images of the whole area (F) and enlargements of the boxed area (G) taken at different time points after photoactivation are shown. See also Movie S1.

(I) Frames from a TIRFM movie showing the behavior of a single PAGFP-Rab8A and mStrawberry-Rab6A-positive vesicle immediately before and during fusion. Time after photoactivation (performed in peripheral cytoplasm using a 407 nm laser) is indicated. See also Movie S2.

(J) Plot of the average fluorescent intensity of moving PAGFP-Rab8A vesicles after photoactivation in the Golgi area. Imaging was performed with a spinning disk microscope. Linescan (line thickness 0.32 μm) was applied to measure pixel intensities along the vesicle path in the kymographs of individual vesicles.

(K) Plot of average fluorescence intensity of a single PAGFP-Rab8A- and mStrawberry-Rab6A-positive vesicle (a circle with a diameter of 0.65 μm) over time. Vesicle appearance in the focal plane is indicated by a vertical arrow. The horizontal arrow points to the peak of fluorescence intensity, corresponding to vesicle fusion with the plasma membrane.

(L) HeLa cells stably expressing NPY-Venus were transfected with the indicated siRNA, fixed, and stained for the endogenous Rab8A 3 days after siRNA transfection. In (A), (B), and (L), insets show enlargements of the boxed areas. Rab8A-positive tubules are indicated by arrows.

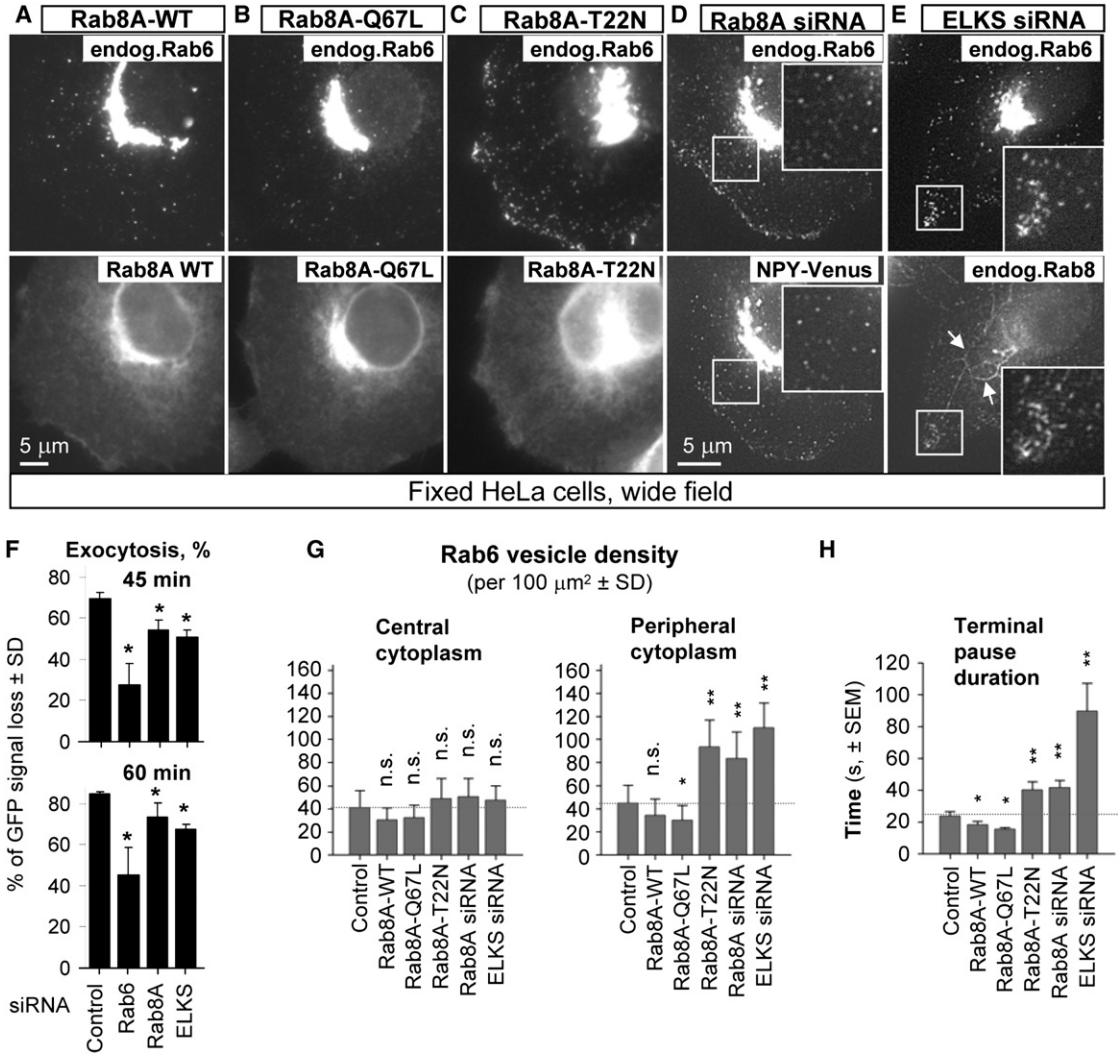

Figure 2. Rab8A Is Required for Docking and Fusion of Rab6 Vesicles

(A–C) HeLa cells were transfected with the indicated GFP-Rab8A fusions and stained for endogenous Rab6.

(D) HeLa cells stably expressing NPY-Venus were transfected with Rab8A siRNA, fixed 3 days later, and stained for endogenous Rab6.

(E) HeLa cells were transfected with ELKS siRNA, fixed 3 days later, and stained for endogenous Rab6 and Rab8A. Tubules positive for Rab8A and negative for Rab6 are indicated by arrowheads. In (D) and (E), insets show enlargements of the boxed areas.

(F) Cells stably expressing the secretion reporter SS-GFP-FM4-FCS-hGH [18] were transfected with different siRNAs; 3 days later, secretion was stimulated by the addition of 1 μM AP21998, and the average intracellular fluorescence was measured using flow cytometry at 45 and 60 min after ligand addition. The percentage of fluorescent signal loss at 45 and 60 min compared to control (no ligand added) was determined in four independent samples for each siRNA and each time point.

(G) Quantification of vesicles positive for endogenous Rab6 in HeLa cells fixed and stained as described for (A)–(E). At least 200 vesicles were analyzed in ~6 cells for each condition.

(H) HeLa cells stably expressing GFP-Rab6A and transfected with the indicated mStrawberry-Rab8A fusions or siRNAs were imaged using wide-field epifluorescence microscopy, and the duration of the pause between vesicle immobilization at the cell periphery and its disappearance was measured. One hundred vesicles in five cells were analyzed for each condition. In (F)–(H), values significantly different from control are indicated by asterisks (*$p < 0.05$; **$p < 0.01$; Mann-Whitney U test).

Using this antibody, we confirmed the interaction between endogenous MICAL3 and ELKS (Figure 3C). In contrast, we observed no strong interaction between ELKS and MICAL1, a conclusion supported by pull-downs of BioGFP-MICAL1 and BioGFP-MICAL3 (Figure S3E). Furthermore, using pull-down assays from cells expressing BioGFP-ELKS together with different MICAL3 fragments, we mapped the ELKS-interacting domain to the C-terminal portion of MICAL3 (MICAL3-C2) that is distinct from Rab8A-binding region MICAL3-CC (Figures 3A and 3D; Figure S3F). Using ELKS deletion mutants, we found that MICAL3- and Rab6-interacting regions on ELKS are also distinct: the sequence between amino acids 950 and 1015 of ELKS is required for Rab6, but not for MICAL3 binding (Figures 3E and 3G; Figure S3G).

Next, we investigated whether Rab8A, ELKS, and MICAL3 could form a triple complex in transfected cells and found that FLAG-tagged Rab8A coprecipitated GFP-ELKS more efficiently when it was coexpressed together with GFP-MICAL3 (Figure 3F). Coprecipitation was specific for Rab8A, because it was not observed with Rab7 (Figure S3H). We conclude

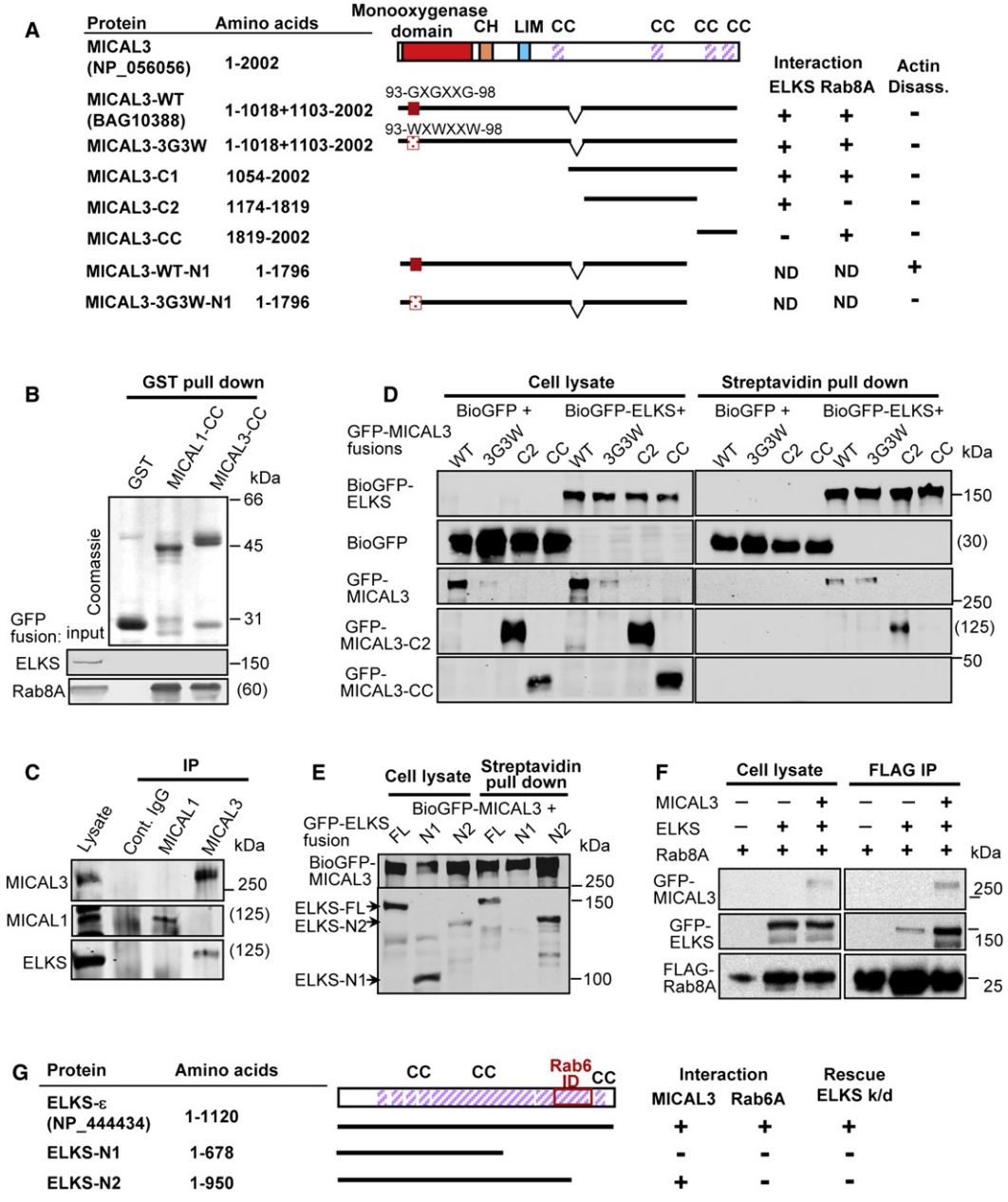

Figure 3. MICAL3 Binds to Rab8A and ELKS

(A) A scheme of MICAL3 protein and the constructs used in this study and a summary of identified interactions (ND, not determined). The accession numbers of the protein sequences used are indicated. The numbering is based on MICAL3 isoform 1 (NCBI protein NP_056056); compared to this sequence, the full-length clone used in this study contains a short internal deletion that does not affect any of the conserved domains. Abbreviations for protein domains: CH, calponin homology domain; LIM, Lin11, Isl-1, and Mec-3 domain (zinc binding); CC, predicted coiled coil. Actin disassembly was determined by phalloidin staining in transfected cells; see Figure S4F.

(B) GST pull-down assays were performed with the indicated GST fusions and lysates of cells expressing GFP-ELKS or GFP-Rab8A. Coomassie-stained gels are shown for GST fusions and western blots with anti-GFP antibodies for GFP fusions. Calculated molecular mass is indicated in parentheses in cases where it is not possible to show the marker position.

(C) Immunoprecipitations (IPs) from HeLa cell extracts with control rabbit IgG or antibodies against MICAL1 or MICAL3 were analyzed by western blotting with the indicated antibodies.

(D and E) Streptavidin pull-down assays from extracts of HEK293T cells coexpressing BirA, BioGFP, or BioGFP-ELKS and the indicated GFP-MICAL3 fusions (D) or BioGFP-MICAL3 and the indicated GFP-ELKS fusions (E). In (D), all proteins were detected with anti-GFP antibodies; in (E), BioGFP-MICAL3 was detected with anti-GFP antibodies and ELKS fusions with the antibodies against ELKS N terminus. In experiments shown in (B)–(E), 2% of the input and 10% of the precipitate was loaded on gel.

(F) IPs from HEK293T cells coexpressing the indicated constructs using anti-FLAG antibodies. Western blotting was performed with antibodies against GFP or the FLAG tag. For the blots with anti-GFP antibodies, 7% of the input and 40% of the precipitate was loaded on gel; for blots with anti-FLAG antibodies, 7% of input and precipitate was loaded.

(G) A scheme of ELKS protein and the constructs used in this study and a summary of their functional properties. CC, coiled coil; Rab6 ID, Rab6 interaction domain [20]; rescue ELKS k/d, reversal of Rab6 vesicle accumulation in ELKS-depleted cells [1].

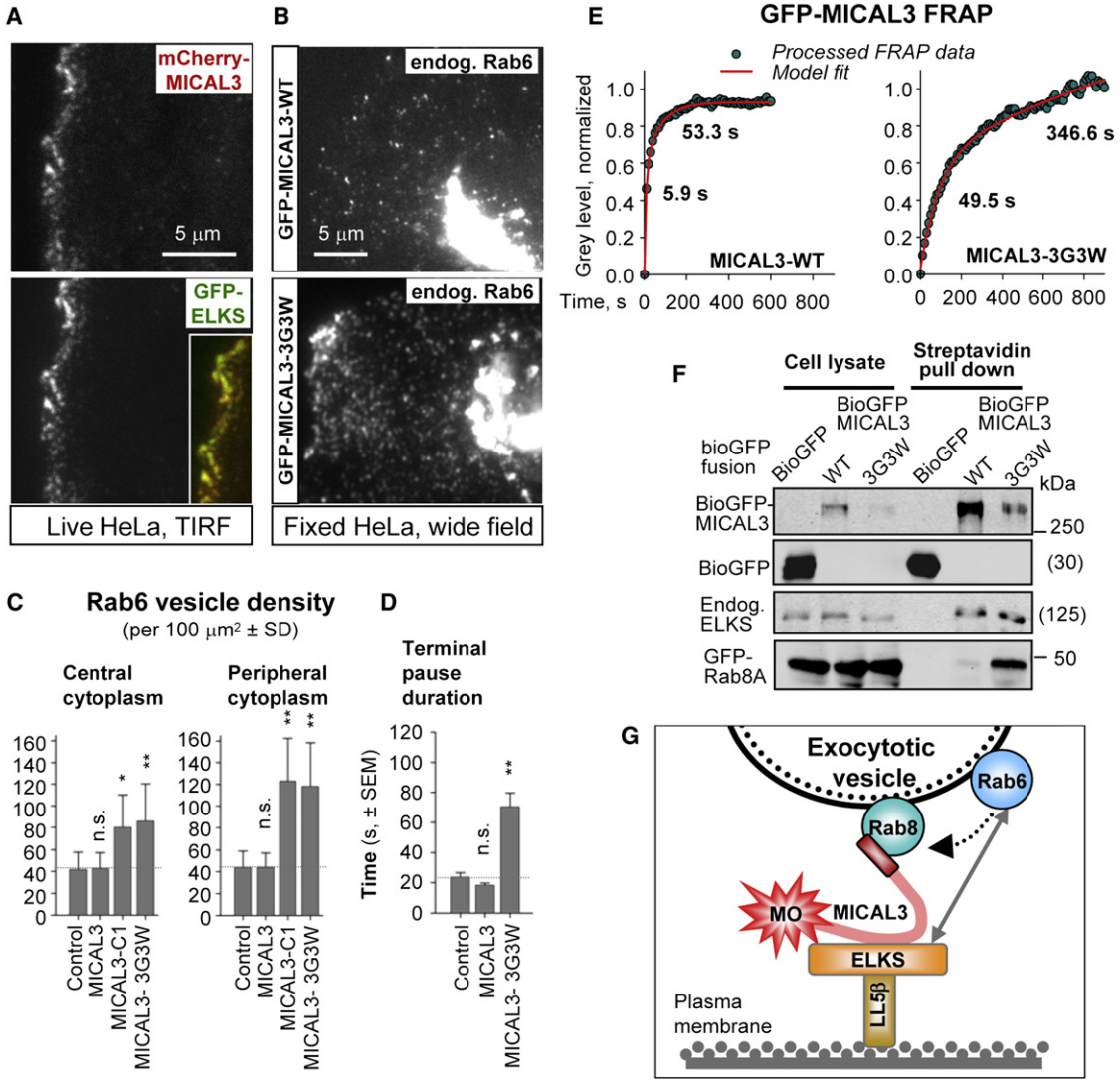

Figure 4. MICAL3 Is Involved in Rab6 Vesicle Fusion with the Plasma Membrane

(A) Analysis of colocalization of mCherry-MICAL3 with the indicated GFP fusions at low expression levels in live HeLa cells using TIRFM. Insets show overlays of the two channels, with GFP signal in green and mCherry in red.

(B) HeLa cells expressing the indicated GFP-MICAL3 fusions were fixed and stained for endogenous Rab6.

(C) Quantification of vesicles positive for endogenous Rab6 in HeLa cells as described for Figure 2G.

(D) Duration of the pause between vesicle immobilization at the cell periphery and its disappearance measured in HeLa cells stably expressing GFP-Rab6A and transiently transfected with mCherry-MICAL3-3G3W. Analysis was performed as described for Figure 2H. In (C) and (D), values significantly different from control are indicated by asterisks (*$p < 0.05$; **$p < 0.01$; Mann-Whitney U test).

(E) Analysis of GFP-MICAL3 and GFP-MICAL3-3G3W turnover by FRAP. The plots show processed FRAP data (green dots) and their fitting to a two-exponential model (red lines); see Supplemental Experimental Procedures and Table S1 for details. Eleven or twelve cells were analyzed in three experiments. The recovery half-times for the two components are indicated.

(F) Streptavidin pull-down assays from extracts of HEK293T cells coexpressing GFP-Rab8A, BirA, BioGFP, or the indicated BioGFP-MICAL3 fusions. All GFP proteins were detected with anti-GFP antibodies and endogenous ELKS with antibodies against ELKS C terminus. Two percent of the input and 10% of the precipitate was loaded on gel. Calculated molecular mass is indicated in parentheses in cases where it is not possible to show the marker position.

(G) A model for cooperative action of Rab6 and Rab8A in exocytosis. Rab6 promotes recruitment of Rab8A to the vesicles. Rab8A interacts with ELKS-positive cortical sites through MICAL3, which binds to ELKS. Rab6 also contributes to vesicle interactions with the cortex through direct binding to ELKS. Redox activity of MICAL3 promotes the docking-complex remodeling and vesicle fusion.

that MICAL3 can promote the interaction between Rab8A and ELKS. Importantly, the ELKS-N2 mutant, which can bind to MICAL3 but not to Rab6 (Figure 3G), cannot rescue the phenotype of ELKS depletion [1], indicating that the direct ELKS-Rab6 interaction appears functionally important in spite of the existence of an additional link between ELKS and the secretory vesicles provided by the MICAL3-Rab8 complex.

Fluorescently tagged MICAL3 localized to the nucleus and cytoplasm; it could be found on Rab8A-positive tubules, the size and number of which increased when both MICAL3 and Rab8A were highly overexpressed (Figure S4A). Using TIRFM in live cells, we could clearly detect MICAL3 in ELKS-positive patches at the cell cortex (Figure 4A). Endogenous MICAL3 was also found at the cortical patches where ELKS and its

cortical partner LL5β were accumulated (Figure S4B). We observed frequent immobilization and fusion of Rab6A- and Rab8A-labeled vesicles at the sites of cortical accumulation of MICAL3 (Figure S4C and data not shown).

We were unable to fully deplete MICAL3 (Figure S3D), and partial MICAL3 knockdown had no clear effect on Rab6 vesicle behavior. As an alternative, we generated a dominant-negative MICAL3 mutant, in which the three glycines in the FAD binding motif GXGXXG were mutated to tryptophans (the 3G3W mutant, Figure 3A). This triple mutation was shown to abrogate the function of *Drosophila* Mical in axon guidance and actin disassembly [22, 23]. Expression of MICAL3-3G3W, but not the wild-type MICAL3, dramatically increased the number of secretory vesicles positive for Rab6 and NPY-Venus (Figures 4B and 4C; Figure S4D). Live-cell imaging showed that these vesicles underwent rapid docking and became immobilized but failed to fuse with the plasma membrane for long time periods (Figure 4D; Figures S2G and S4E), suggesting that MICAL3 helps to attach Rab8-bound vesicles to the cortex, but, without the monooxygenase activity, subsequent fusion steps are inhibited.

The monooxygenase activity of *Drosophila* Mical is used to disassemble actin filaments [23]. We overexpressed the N-terminal part of MICAL3 and found that it strongly reduced the amount of filamentous actin in cells, an effect that was dependent on the intact monooxygenase domain (Figure S4F). The expression of the full-length protein showed no strong effect on actin, possibly as a result of autoinhibition by the C-terminal domain [26]. It is therefore possible that during vesicle fusion, activated MICAL3 promotes disassembly of the cortical actin. In line with this view, MICAL3-3G3W overexpression caused appearance of an actin pool with slow turnover (Figure S4G; Table S1). However, actin disassembly by latrunculin B did not prevent vesicle accumulation induced by the expression of MICAL3-3G3W (data not shown). Moreover, expression of MICAL3-C1, which lacks not only the monooxygenase activity but also the actin-binding CH domain (Figure 3A), caused a strong vesicle accumulation similar to that caused by MICAL3-3G3W (Figure 4C).

To explain these observations, we hypothesized that the redox function of MICAL3 might be needed to destabilize protein complexes in which it is engaged. In line with this view, we found that the turnover of MICAL3 at the cell cortex was much slower for the monooxygenase-deficient MICAL3-3G3W mutant as compared to the wild-type protein (Figure 4E; Table S1). Furthermore, although MICAL3-3G3W showed lower expression and was more difficult to precipitate than MICAL3-WT, it pulled down the same amount of ELKS and a larger amount of Rab8A than the wild-type protein, suggesting that its interaction with the binding partners is increased (Figure 4F). We propose that the redox activity of MICAL3 promotes vesicle fusion by remodeling vesicle-docking complexes in which it is engaged.

In this study, we showed that representatives of two highly conserved Rab families, Rab6 and Rab8, cooperate in control of exocytotic vesicle behavior. Crosstalk between different Rabs in regulation of adjacent trafficking stages was previously demonstrated for exocytosis as well as for endosomal Rabs [27, 28]. Here we provide an example of when two Rabs act simultaneously on the same vesicle, but have different functions: Rab6 controls Rab8A recruitment, vesicle transport, and the choice of fusion sites [1], while Rab8A promotes efficient vesicle docking and fusion, in agreement with the role of Rab8 homolog in yeast [27]. It is possible that a system dependent on two Rabs has evolved by convergence of two initially separate pathways, one controlling plasma membrane fusion (Rab8) and the other regulating the emergence and movement of Golgi-derived carriers (Rab6).

Participation of Rab8A in vesicle fusion with the plasma membrane might represent its general function, which might require interactions with actin-based motors [12, 29] or components of vesicle tethering and fusion machinery, such as the exocyst or SNAREs [27]. We provide evidence that this function is also associated with binding to the MICAL-family proteins (Figure 4G). The two mammalian MICAL-like (MICAL-L1/L2) family members, which lack the redox activity, were already implicated in vesicle trafficking [24, 30], and the *Mical* fly gene was found as a hit in a screen for secretory pathway components [31]. Our results suggest that the enzymatically active MICAL proteins can participate in vesicle tethering and fusion, most likely by monooxygenase-dependent disassembly of protein complexes.

Supplemental Information

Supplemental Information includes four figures, one table, Supplemental Experimental Procedures, and two movies and can be found with this article online at doi:10.1016/j.cub.2011.04.030.

Acknowledgments

We are grateful to A. Peden, A. Barnekow, I. Kaverina, J. Sanes, R. Tsien, A. Miyawaki, F. Melchior, and I. Mellman for the gift of materials and to G. Schaaf, R. van der Linden, and E. Dzierzak for the use of fluorescence-activated cell sorting (FACS) equipment. This work was supported by a Netherlands Organization for Health Research (ZonMW) TOP grant and the Netherlands Organization for Scientific Research (NWO) ALW-VICI grants to A.A.; by a Fundação para a Ciência e a Tecnologia fellowship to A.S.-M.; by NWO-ALW, NWO-CW, and ZonMW-VIDI grants and a ESF-EURYI award to C.C.H.; the ZonMW-VIDI and the Human Frontier Science Program (Career Development Awards) to R.J.P.; and a NWO-CW ECHO grant to P.v.d.S.

Received: October 10, 2010
Revised: March 16, 2011
Accepted: April 18, 2011
Published online: May 19, 2011

References

1. Grigoriev, I., Splinter, D., Keijzer, N., Wulf, P.S., Demmers, J., Ohtsuka, T., Modesti, M., Maly, I.V., Grosveld, F., Hoogenraad, C.C., and Akhmanova, A. (2007). Rab6 regulates transport and targeting of exocytotic carriers. Dev. Cell *13*, 305–314.
2. Ang, A.L., Folsch, H., Koivisto, U.M., Pypaert, M., and Mellman, I. (2003). The Rab8 GTPase selectively regulates AP-1B-dependent basolateral transport in polarized Madin-Darby canine kidney cells. J. Cell Biol. *163*, 339–350.
3. Huber, L.A., Pimplikar, S., Parton, R.G., Virta, H., Zerial, M., and Simons, K. (1993). Rab8, a small GTPase involved in vesicular traffic between the TGN and the basolateral plasma membrane. J. Cell Biol. *123*, 35–45.
4. Sato, T., Mushiake, S., Kato, Y., Sato, K., Sato, M., Takeda, N., Ozono, K., Miki, K., Kubo, Y., Tsuji, A., et al. (2007). The Rab8 GTPase regulates apical protein localization in intestinal cells. Nature *448*, 366–369.
5. Hattula, K., Furuhjelm, J., Tikkanen, J., Tanhuanpaa, K., Laakkonen, P., and Peranen, J. (2006). Characterization of the Rab8-specific membrane traffic route linked to protrusion formation. J. Cell Sci. *119*, 4866–4877.
6. Kolk, S.M., and Pasterkamp, R.J. (2007). MICAL flavoprotein monooxygenases: Structure, function and role in semaphorin signaling. Adv. Exp. Med. Biol. *600*, 38–51.
7. Martinez, O., Schmidt, A., Salamero, J., Hoflack, B., Roa, M., and Goud, B. (1994). The small GTP-binding protein rab6 functions in intra-Golgi transport. J. Cell Biol. *127*, 1575–1588.

8. White, J., Johannes, L., Mallard, F., Girod, A., Grill, S., Reinsch, S., Keller, P., Tzschaschel, B., Echard, A., Goud, B., and Stelzer, E.H. (1999). Rab6 coordinates a novel Golgi to ER retrograde transport pathway in live cells. J. Cell Biol. *147*, 743–760.
9. Del Nery, E., Miserey-Lenkei, S., Falguieres, T., Nizak, C., Johannes, L., Perez, F., and Goud, B. (2006). Rab6A and Rab6A′ GTPases play non-overlapping roles in membrane trafficking. Traffic *7*, 394–407.
10. Opdam, F.J., Echard, A., Croes, H.J., van den Hurk, J.A., van de Vorstenbosch, R.A., Ginsel, L.A., Goud, B., and Fransen, J.A. (2000). The small GTPase Rab6B, a novel Rab6 subfamily member, is cell-type specifically expressed and localised to the Golgi apparatus. J. Cell Sci. *113*, 2725–2735.
11. Nagai, T., Ibata, K., Park, E.S., Kubota, M., Mikoshiba, K., and Miyawaki, A. (2002). A variant of yellow fluorescent protein with fast and efficient maturation for cell-biological applications. Nat. Biotechnol. *20*, 87–90.
12. Roland, J.T., Kenworthy, A.K., Peranen, J., Caplan, S., and Goldenring, J.R. (2007). Myosin Vb interacts with Rab8a on a tubular network containing EHD1 and EHD3. Mol. Biol. Cell *18*, 2828–2837.
13. Nachury, M.V., Loktev, A.V., Zhang, Q., Westlake, C.J., Peranen, J., Merdes, A., Slusarski, D.C., Scheller, R.H., Bazan, J.F., Sheffield, V.C., and Jackson, P.K. (2007). A core complex of BBS proteins cooperates with the GTPase Rab8 to promote ciliary membrane biogenesis. Cell *129*, 1201–1213.
14. Patterson, G.H., and Lippincott-Schwartz, J. (2002). A photoactivatable GFP for selective photolabeling of proteins and cells. Science *297*, 1873–1877.
15. Toomre, D., Steyer, J.A., Keller, P., Almers, W., and Simons, K. (2000). Fusion of constitutive membrane traffic with the cell surface observed by evanescent wave microscopy. J. Cell Biol. *149*, 33–40.
16. Hattula, K., Furuhjelm, J., Arffman, A., and Peranen, J. (2002). A Rab8-specific GDP/GTP exchange factor is involved in actin remodeling and polarized membrane transport. Mol. Biol. Cell *13*, 3268–3280.
17. Luo, H.R., Saiardi, A., Nagata, E., Ye, K., Yu, H., Jung, T.S., Luo, X., Jain, S., Sawa, A., and Snyder, S.H. (2001). GRAB: A physiologic guanine nucleotide exchange factor for Rab3A, which interacts with inositol hexakisphosphate kinase. Neuron *31*, 439–451.
18. Gordon, D.E., Bond, L.M., Sahlender, D.A., and Peden, A.A. (2010). A targeted siRNA screen to identify SNAREs required for constitutive secretion in mammalian cells. Traffic *11*, 1191–1204.
19. Miserey-Lenkei, S., Chalancon, G., Bardin, S., Formstecher, E., Goud, B., and Echard, A. (2010). Rab and actomyosin-dependent fission of transport vesicles at the Golgi complex. Nat. Cell Biol. *12*, 645–654.
20. Monier, S., Jollivet, F., Janoueix-Lerosey, I., Johannes, L., and Goud, B. (2002). Characterization of novel Rab6-interacting proteins involved in endosome-to-TGN transport. Traffic *3*, 289–297.
21. Lansbergen, G., Grigoriev, I., Mimori-Kiyosue, Y., Ohtsuka, T., Higa, S., Kitajima, I., Demmers, J., Galjart, N., Houtsmuller, A.B., Grosveld, F., and Akhmanova, A. (2006). CLASPs attach microtubule plus ends to the cell cortex through a complex with LL5beta. Dev. Cell *11*, 21–32.
22. Terman, J.R., Mao, T., Pasterkamp, R.J., Yu, H.H., and Kolodkin, A.L. (2002). MICALs, a family of conserved flavoprotein oxidoreductases, function in plexin-mediated axonal repulsion. Cell *109*, 887–900.
23. Hung, R.J., Yazdani, U., Yoon, J., Wu, H., Yang, T., Gupta, N., Huang, Z., van Berkel, W.J., and Terman, J.R. (2010). Mical links semaphorins to F-actin disassembly. Nature *463*, 823–827.
24. Yamamura, R., Nishimura, N., Nakatsuji, H., Arase, S., and Sasaki, T. (2008). The interaction of JRAB/MICAL-L2 with Rab8 and Rab13 coordinates the assembly of tight junctions and adherens junctions. Mol. Biol. Cell *19*, 971–983.
25. Fukuda, M., Kanno, E., Ishibashi, K., and Itoh, T. (2008). Large scale screening for novel rab effectors reveals unexpected broad Rab binding specificity. Mol. Cell. Proteomics *7*, 1031–1042.
26. Schmidt, E.F., Shim, S.O., and Strittmatter, S.M. (2008). Release of MICAL autoinhibition by semaphorin-plexin signaling promotes interaction with collapsin response mediator protein. J. Neurosci. *28*, 2287–2297.
27. Novick, P., Medkova, M., Dong, G., Hutagalung, A., Reinisch, K., and Grosshans, B. (2006). Interactions between Rabs, tethers, SNAREs and their regulators in exocytosis. Biochem. Soc. Trans. *34*, 683–686.
28. Rink, J., Ghigo, E., Kalaidzidis, Y., and Zerial, M. (2005). Rab conversion as a mechanism of progression from early to late endosomes. Cell *122*, 735–749.
29. Sahlender, D.A., Roberts, R.C., Arden, S.D., Spudich, G., Taylor, M.J., Luzio, J.P., Kendrick-Jones, J., and Buss, F. (2005). Optineurin links myosin VI to the Golgi complex and is involved in Golgi organization and exocytosis. J. Cell Biol. *169*, 285–295.
30. Sharma, M., Giridharan, S.S., Rahajeng, J., Naslavsky, N., and Caplan, S. (2009). MICAL-L1 links EHD1 to tubular recycling endosomes and regulates receptor recycling. Mol. Biol. Cell *20*, 5181–5194.
31. Wendler, F., Gillingham, A.K., Sinka, R., Rosa-Ferreira, C., Gordon, D.E., Franch-Marro, X., Peden, A.A., Vincent, J.P., and Munro, S. (2010). A genome-wide RNA interference screen identifies two novel components of the metazoan secretory pathway. EMBO J. *29*, 304–314.